https://doi.org/10.5194/acp-2019-607
Preprint. Discussion started: 28 August 2019

Atmospheric Chemistry and Physics
Discussions

Supercooled Liquid Water Clouds observed and analysed at the Top of the Planetary Boundary Layer above Dome C, Antarctica

Philippe Ricaud[1], Massimo Del Guasta[2], Eric Bazile[1], Niramson Azouz[1], Angelo Lupi[3], Pierre Durand[4], Jean-Luc Attié[4], Dana Veron[5], Vincent Guidard[1] and Paolo Grigioni[6]

[1]CNRM, Université de Toulouse, Météo-France, CNRS, Toulouse, France
[2]INO-CNR, Sesto Fiorentino, Italy
[3]ISAC-CNR, Italy
[4]Laboratoire d'Aérologie, Université de Toulouse, CNRS, UPS, Toulouse, France
[5]University of Delaware, Newark, USA
[6]ENEA, Roma, Italy

https://doi.org/10.5194/acp-2019-607
Preprint. Discussion started: 28 August 2019

Abstract

A comprehensive analysis of the water budget over the Dome C (Concordia, Antarctica) station has been performed during the austral summer 2018-2019 as part of the Year of Polar Prediction (YOPP) international campaign. Thin (~100-m) supercooled liquid water (SLW) clouds have been detected and analysed using remotely sensed observations at the station (tropospheric depolarization LIDAR, microwave radiometer HAMSTRAD, net surface radiation from Baseline Surface Radiation Network, BSRN), radiosondes and using satellite observations (CALIOP/CALIPSO) combined with a specific configuration of the Numerical Weather Prediction model: ARPEGE-SH. Two case studies are used to illustrate this phenomenon. On 24 December 2018, the atmospheric planetary boundary layer (PBL) evolved following a "typical" diurnal variation, that is to say with a warm and dry mixing layer at local noon thicker than the cold and dry stable layer at local midnight. Our study showed that the SLW clouds were observed at Dome C within the entrainment and the capping inversion zones at the top of the PBL. ARPEGE-SH was not able to correctly estimate the ratio between liquid and solid water inside the clouds. The SLW content was always strongly underestimated in the studied cases. The lack of simulated SLW in the model impacted the net surface radiation that was 20-30 W m^{-2} higher in the BSRN observations than in the ARPEGE-SH calculations, mainly attributable to longwave downward surface radiation from BSRN being 50 W m^{-2} greater than that of ARPEGE-SH. On 20 December 2018, a warm and wet episode impacted the PBL with no clear diurnal cycle of the PBL top. SLW cloud appearance coincided with the warm and wet event within the entrainment and capping inversion zones. The amount of liquid water measured by HAMSTRAD was ~20 times greater in this perturbed PBL than in the "typical" PBL. Since ARPEGE-SH was not able to accurately reproduce these SLW clouds, the discrepancy between the observed and calculated net surface radiation was even greater than in the "typical" PBL period, reaching +50 W m^{-2}, mainly attributable to longwave downward surface radiation from

https://doi.org/10.5194/acp-2019-607
Preprint. Discussion started: 28 August 2019

Atmospheric Chemistry and Physics Discussions

BSRN being 100 W m^{-2} greater than that of ARPEGE-SH. The absence of SLW clouds in NWPs over Antarctica may indicate an incorrect simulation of the radiative budget of the polar atmosphere.

https://doi.org/10.5194/acp-2019-607
Preprint. Discussion started: 28 August 2019

Atmospheric Chemistry and Physics Discussions

1. Introduction

Antarctic clouds play an important role in the climate system by influencing the Earth's radiation balance, both directly at high southern latitudes and, indirectly, at the global level through complex teleconnections (Lubin et al., 1998). In Antarctica, there are very few observational stations and most of them are located on the coast, a fact that limits the type and characteristics of clouds observed. Nevertheless, prior studies suggest that cloud properties vary geographically, with a fractional cloud cover around the South Pole of about 50 to 60% in all seasons, and a cloud cover of about 80 to 90% near the coast (Bromwich et al., 2012). Based on spaceborne observations (Adhikari et al., 2012), the Antarctic Plateau has the lowest cloud occurrence of the Antarctic continent (<30%). Furthermore, cloud parameters such as the hydrometeors size and the microphysical structure are also very difficult to retrieve in Antarctica. Nevertheless, some measurements exist showing that ice crystal clouds are mainly observed inland with crystal sizes ranging from 5 to 30 μm (effective radius) in the core of the cloud; mixed-phase clouds are preferably observed near the coast with slightly larger ice crystals and water droplets (Lachlan-Cope, 2010).

The time and geographical distribution of tropospheric clouds above the whole Antarctic continent has been recently studied using the raDAR/liDAR-MASK (DARDAR) spaceborne products (Listowski et al., 2018). The authors determined that clouds are mainly constituted of ice above the continent. The presence of Supercooled Liquid Water (SLW, the water staying in liquid phase below 0°C) clouds shows variations according to temperature and sea ice fraction, decreasing sharply poleward, with an abundance two to three times less over the Eastern Antarctic Plateau than over the Western Antarctic. The difficulty of mesoscale high-resolution models and operational numerical weather prediction models to accurately calculate the net surface radiation due to the presence of clouds (particularly of SLW clouds) in Antarctica

https://doi.org/10.5194/acp-2019-607
Preprint. Discussion started: 28 August 2019

causes biases of several tens of watt per square meters (King et al., 2006; Bromwich et al., 2013) impacting the Earth's radiative budget (Lawson and Gettelman, 2014).

With the support of the World Meteorological Organization (WMO) World Weather Research Programme (WWRP), the Polar Prediction Project (PPP) international programme has been dedicated to the development of improved weather and environmental prediction services for the polar regions, on time scales from hours to seasons (https://www.polarprediction.net). Within this project, the Year of Polar Prediction (YOPP), from 2018 to 2019, aims at enabling a significant improvement in environmental prediction capabilities for the polar regions and beyond, by coordinating a period of intensive observing, modelling, verification, user-engagement and educational activities. The Water Budget over Dome C (H_2O-DC) project has been endorsed by YOPP for studying the water budget by means of ground-based measurements of water (vapour, solid and liquid) and clouds, by active (backscatter LIDAR) and passive (microwave radiometer) remote sensing, and operational meteorological analyses. The Dome C (Concordia) station is located in the Eastern Antarctic Plateau (75°06'S, 123°21'E, 3233 m above mean sea level, amsl).

H_2O-DC concentrates on the Special Observing Period (SOP) of measurements in the Antarctic, from 16 November 2018 to 15 February 2019. During this time frame, several instruments have been employed.

1) The H_2O Antarctica Microwave Stratospheric and Tropospheric Radiometer (HAMSTRAD) radiometer (Ricaud et al., 2010a) to obtain vertical profiles of temperature and water vapour, Integrated Water Content (IWC) or precipitable water, and Liquid Water Path (LWP), with an adjustable time resolution better than 7 minutes.

2) The tropospheric depolarization LIDAR (Tomasi et al., 2015) to obtain vertical profiles of backscattering and depolarization.

These two H_2O-DC data sets have been complemented in the present analysis by the 3 following observational datasets.

3) The Baseline Surface Radiation Network (BSRN) net surface radiances at the station.

4) The temperature profiles from radiosondes launched twice daily at the station during YOPP.

5) The spaceborne observations (backscatter and polarization) from the CALIOP/CALIPSO LIDAR in the vicinity of the station.

In addition, a specific configuration of the global ARPEGE model from Météo-France (Pailleux et al., 2015) is used to characterize the water budget above Dome C considering the gas, liquid and the solid phases to study the genesis of clouds (ice/liquid).

The aim of the present study is to combine all these observations and simulations in order to 1) detect the presence of SLW clouds above Dome C, 2) analyse the formation and evolution of such SLW clouds and 3) estimate the radiative impact of such clouds on the net surface radiation. We concentrate the analyses on two case studies observed during the YOPP campaign: one case when the Planetary Boundary Layer (PBL) exhibited a “typical” diurnal cycle (24 December 2018) and a second case when the diurnal cycle of the PBL was perturbed by a warm and wet episode (20 December 2018).

The data sets used in our study are presented in section 2. The analyses of the SLW clouds during the typical and the perturbed PBL periods are detailed in sections 3 and 4, respectively. A conclusion synthetizes the study in section 5.

2. Datasets

2.1. The HAMSTRAD Radiometer

HAMSTRAD is a microwave radiometer to probe water vapour (H_2O), liquid water and tropospheric temperature above Dome C. Measuring at 60 GHz (oxygen molecule line (O_2) to

https://doi.org/10.5194/acp-2019-607
Preprint. Discussion started: 28 August 2019

deduce the temperature) and at 183 GHz (H_2O line), this unique, state-of-the-art radiometer was installed on site for the first time in January 2009 (Ricaud et al., 2010a). The measurements of the HAMSTRAD radiometer allow the retrieval of the vertical profiles of H_2O and temperature from the ground to 10 km altitude with a temporal resolution of 7 minutes and vertical resolutions of 30 to 50 m in the atmospheric boundary layer, 100 m in the free troposphere and 500 m in the upper troposphere-lower stratosphere. The temporal resolution on the instrument allows for detection and analysis of atmospheric processes such as the diurnal evolution of the PBL (Ricaud et al., 2012) and the presence of clouds and diamond dust (Ricaud et al., 2017). In addition, two other parameters can be estimated.

1) The Integrated Water Vapour (IWV) or precipitable water (kg m^{-2}) obtained by integrating the absolute humidity profile from the surface to 10 km altitude.

2) The Liquid Water Path (kg m^{-2}) that gives the amount of liquid water integrated along the vertical.

IWV has been validated against radiosondes at Dome C between 2010 and 2014 showing a 5-10% wet bias of HAMSTRAD compared to the sondes (Ricaud et al., 2015). LWP has only been studied when the instrument was installed at the Pic du Midi station (2877 amsl, France) during the calibration/validation period in 2008 prior to its set up in Antarctica in 2009 (Ricaud et al., 2010b).

2.2. The tropospheric depolarization LIDAR

A tropospheric depolarization LIDAR (532 nm) has been operating at Dome C since 2008 (see http://lidarmax.altervista.org/englidar/_Antarctic%20LIDAR.php). The LIDAR provides 5-min tropospheric profiles of aerosols and clouds continuously, from 20 to 7000 m amsl, with a resolution of 7.5 m. LIDAR depolarization (Mishchenko et al., 2000) is a robust indicator of non-spherical shape for randomly oriented cloud particles. A depolarization ratio below 10% is

https://doi.org/10.5194/acp-2019-607
Preprint. Discussion started: 28 August 2019

Atmospheric Chemistry and Physics Discussions

characteristic of SLW clouds, while higher values are produced by ice particles. The possible ambiguity between SLW clouds and oriented ice plates is avoided at Dome C by operating the LIDAR 4° off-zenith (Hogan and Illingworth, 2003). The LIDAR observations at Dome C have already been used to study the radiative properties of water vapour and clouds in the far infrared (Palchetti et al., 2015). As a support to LIDAR data interpretation, time-lapse webcam videos of local sky conditions are also collected.

2.3. The BSRN Network

At the Astroconcordia/Albedo-Rack sites, the upward and downward looking, heated and ventilated standard Kipp&Zonen CM22 pyranometers and infrared CG4 pyrgeometers provide measurements of hemispheric downward and upward broadband shortwave (SW, 0.3–3 μm) and longwave (LW, 4–50 μm) fluxes at the surface, respectively. These data are used to retrieve values of net surface radiation (defined as the difference between the downward and upward fluxes). All these measurements follow the rules of acquisition, quality check and quality control of the BSRN as described in Driemel et al. (2018).

2.4. Radiosondes

Vertical temperature and humidity profiles have been measured on a daily basis at Dome C since 2005, employing RS92 radiosondes using Vaisala standard evaluation programs. The sondes are known to have a cold bias of 1.2 K from the ground to about 4 km altitude (Tomasi et al., 2011 and 2012). During YOPP and the two case studies, launches were performed twice per day at 00:00 and 12:00 UTC.

2.5. CALIOP onboard CALIPSO

Orbiting at 705-km altitude, the CALIPSO (Cloud Aerosol Lidar and Infrared Pathfinder Satellite Observations) mini-satellite has been observing clouds and aerosols since 2006 to better understand the role of clouds and aerosols in climate. To accomplish this mission, the CALIPSO satellite is equipped with a LIDAR, a camera and an infrared imager (Winker et al., 2009). CALIOP (Cloud-Aerosol LIdar with Orthogonal Polarization) is a dual-wavelength (532 and 1064 nm) backscatter LIDAR. It provides high-resolution vertical profiles of clouds and aerosols along the orbit track (Young et al., 2009).

2.6. The specific ARPEGE-SH Model

A specific configuration of the operational global model ARPEGE was used for the YOPP Southern Hemisphere (YOPP-SH) period (15/11/2018–15/02/2019). This configuration named ARPEGE-SH is based on the operational global model used for Numerical Weather Prediction (NWP) ARPEGE (Pailleux et al., 2015), but with its highest horizontal resolution centred over Dome C instead of over France, as set up in ARPEGE. A 4D variational (4DVar) assimilation was performed every 6 h. The meteorological analyses were given by the ARPEGE-SH system together with the 24-hour forecasts at the node the closest to the location of Dome C. The horizontal and vertical resolution during the YOPP-SH period were 7.5 km at Dome C, with 105 vertical levels, the first one being set at 10 m. Several ARPEGE-SH output parameters were selected for analysis: cloud fraction, ice, water vapour and liquid-water mixing ratio, temperature, Total Column Ice (TCI, ice integrated along the vertical), LWP, IWV, and net surface radiation.

https://doi.org/10.5194/acp-2019-607
Preprint. Discussion started: 28 August 2019

3. Typical diurnal cycle of the PBL

The first SLW cloud case study occurred on 24 December 2018 over a 24-hour period with a typical diurnal PBL cycle. All the results are presented in Universal Time Coordinated (UTC) with local time (LT) being eight hours ahead of UTC (LT = UTC + 8).

3.1. Clouds

The presence of clouds is highlighted by the LIDAR backscatter and depolarization profiles shown in Figures 1a and b, respectively. High values of LIDAR cloud backscatter ($\beta_c > 100$ β_{mol}, with β_{mol} the molecular backscatter), indicate that clouds and/or precipitation are present over the whole day with some significant differences. First, vertical "stripes" of high backscatter values are visible from 10 to 400 m height before 10:00 UTC and after 19:00 UTC, associated with high values of depolarization ratio (> 20 %), characteristic of precipitating ice crystals. Second, high values of β_c associated with very low depolarization ratio (< 5 %) occur within a thin layer of approximately 100-m depth around 500 m from 08:00 to 22:00 UTC, with some breaks around 11:00 and 19:00-21:00 UTC. From the LIDAR observations, this combination of high backscatter and low depolarization ratio signifies the presence of a SLW cloud (Figure 1c).

The NWP model ARPEGE-SH calculates cloud fraction, ice water and liquid water mixing ratios (kg kg^{-1}) for 24 December 2018 (Figures 2a, b and c, respectively). We note that the outputs from ARPEGE-SH at 00:00 and 12:00 UTC are the analyses and, for the remaining time, the outputs are the hourly forecasts. ARPEGE-SH predicts the presence of clouds (cloud fraction > 0.95) for most of the day except around 11:00 and 23:00 UTC (Fig. 2a). Before 12:00 UTC, the clouds are mainly confined between 300 and 600-800 m whilst, after 12:00 UTC, they spread from the surface to 800 m. There are also high-level clouds at 2000-3000 m height but with a cloud fraction between 0.50 and 0.70. The majority of the clouds produced by

https://doi.org/10.5194/acp-2019-607
Preprint. Discussion started: 28 August 2019

Atmospheric Chemistry and Physics
Discussions

ARPEGE-SH are mainly composed of ice crystals (Fig. 2b) with some traces of droplets (Fig. 2c). The ice/liquid water clouds derived from the LIDAR observations are superimposed over the SLW clouds calculated by ARPEGE-SH. It is obvious that ARPEGE-SH fails in estimating both the vertical distribution of liquid water (a thin layer is observed around 500 m whereas the modelled cloud layer extends from the surface to 800 m) and its temporal evolution (presence of SLW cloud almost all day long in ARPEGE-SH compared to SLW clouds from 08:00 to 22:00 UTC in the observations).

The presence of clouds above the station can also be inferred from vertically-integrated variables such as: 1) TCI calculated by ARPEGE-SH, 2) LWP from HAMSTRAD and ARPEGE-SH, and 3) IWV from HAMSTRAD and ARPEGE-SH (Figures 3a, b and c, respectively). The ARPEGE-SH TCI on 24 December 2018 (Fig. 3a) oscillates between 10 and 30 g m^{-2} except around 12:00 UTC when a clear minimum occurs (~3 g m^{-2}), underlining the fact that ARPEGE-SH obtains ice clouds for the entire day, except at 12:00 UTC. The HAMSTRAD LWP shows an obvious increase from ~1.0 to ~2.0-3.0 g m^{-2} when the presence of SLW cloud is indicated by LIDAR observations. The ARPEGE-SH LWP is on average 10^3 times lower than that observed by HAMSTRAD, underlining the fact that ARPEGE-SH misrepresents features of the SLW clouds over Dome C. HAMSTRAD and ARPEGE-SH IWV vary from 0.65-1.05 kg m^{-2} throughout the day on 24 December 2018, with an agreement to within 0.1 kg m^{-2} (i.e. ~10-15%), which is consistent with previous studies (Ricaud et al., 2017). Note that HAMSTRAD IWV is on average 10% higher than IWV inferred from radiosonde observations (Ricaud et al., 2015).

Observation of clouds from space-borne sensors has two main advantages: 1) to validate the nature of the cloud observed over Dome C (namely ice/liquid water), and 2) to estimate the vertical and horizontal extents of the detected cloud. Note that the CALIPSO spaceborne LIDAR operates at the same wavelength as the backscatter LIDAR at Dome C, with the same method for discriminating ice from liquid water. Consequently, the two LIDARs should give consistent information for the detected phase of the clouds. The main difficulty with this approach is related to the time and space sampling of the spaceborne instrument, namely to find a satellite overpass coincident both in time and location with the cloud observed at Dome C. This, unfortunately, decreases the number of overpasses that is scientifically exploitable. Nevertheless, on 24 December 2018, 2 orbits of CALIOP/CALIPSO passed close to Dome C at times when SLW clouds were observed by ground-based instruments. We show the vertical feature mask and ice/water phase from the pass closest to the station, from 15:50 to 16:03 UTC (Figures 4a and b, respectively). Firstly, we note the presence of a cloud a few hundreds of meters deep near the surface in the vicinity of Dome C (Fig. 4a; note that the CALIOP/CALIPSO altitude is above sea level and Dome C is at an altitude of 3233 m amsl). Secondly, this cloud is composed of SLW (Fig. 4b), confirming the analysis based on the observations from the LIDAR and the HAMSTRAD radiometer. Furthermore, we can state that this SLW cloud is not a local phenomenon but is at least 2.5°-latitude wide, namely has a horizontal extent of ~280 km. The other orbit from 14:11 to 14:24 UTC (not shown) is slightly more distant than the one shown in Figure 4, but it exhibits a similar SLW cloud over an even greater horizontal extent of about 5° latitude (~550 km).

3.2. Temperature and water vapour

The presence of SLW clouds in the atmosphere is strongly dependent on the temperature field. From Fig. 2.33 of Pruppacher and Klett (2012), the percentage of clouds containing no ice becomes non-negligible at temperatures greater than -35°C, although SLW clouds have been observed at lower temperatures over Russia (-36°C) and the Rocky Mountains in the USA (-40.7°C). Recent laboratory measurements show that liquid water can exist down to -42.55°C (Goy et al., 2018).

https://doi.org/10.5194/acp-2019-607
Preprint. Discussion started: 28 August 2019

On 24 December 2018, temperatures from both HAMSTRAD and ARPEGE-SH ranged from 240 to 250 K (-33 to -23°C) from the surface to 1-km altitude, compatible with the presence of SLW clouds. The diurnal variations of temperature and water vapour anomalies calculated by ARPEGE-SH and measured by HAMSTRAD are shown in Figure 5. For each altitude, the daily-averaged value has been subtracted. This has the advantages of highlighting areas of maximum and minimum changes along the vertical, and reduces biases when comparing the two data sets. Absolute anomalies (K) are presented for temperatures whilst relative anomalies (%) are shown for water vapour.

The diurnal variation of the ARPEGE-SH temperature (Fig. 5a) from the surface to 1 km amsl shows a warm atmosphere before 12:00 UTC and a fast cooling one afterward. HAMSTRAD shows a similar cooling (Fig. 5b), but the transition is not so abrupt and occurs later, around 15:00 UTC. The diurnal amplitude is greater in ARPEGE-SH (~5 K) than in HAMSTRAD (~3 K). The diurnal variation of the water vapour in ARPEGE-SH (Fig. 5c) from the surface to 1 km shows a wet atmosphere before 12:00 UTC and a drier atmosphere after, again with an abrupt transition. From HAMSTRAD, the diurnal variation of the water vapour (Fig. 5d) from the surface to 1 km is more complex, alternating wet and dry phases, which is particularly obvious at 500-m altitude: wet (00:00-03:00 UTC), dry (03:00-08:00 UTC), wet (08:00-09:00 UTC), dry (09:00-12:00 UTC), wet (12:00-22:00 UTC) and dry (22:00-24:00 UTC). The time evolution of the SLW cloud (Fig. 1c) is superimposed on all the panels of Figure 5.

The diurnal variation of the top of the PBL calculated by ARPEGE-SH (defined as the level where the turbulence kinetic energy becomes lower than 0.01 $m^2 s^{-2}$) is also superimposed on all the panels of Figure 5. We note several key points.

https://doi.org/10.5194/acp-2019-607
Preprint. Discussion started: 28 August 2019

1) The diurnal evolution of the top of the PBL is consistent with previous studies carried out at Dome C (e.g. Argentini et al., 2005; Ricaud et al., 2012; Casasanta et al., 2014), with a top higher when there is a relatively warm mixed layer than in cool stable conditions.

2) The SLW cloud appeared just below the ARPEGE-SH-estimated PBL top, around 08:00 UTC, and persisted around the same altitude after 12:00 UTC even though the top of the PBL had dramatically decreased down to the surface.

3) The SLW cloud persisted after 12:00 UTC in a layer that is wetter and warmer than elsewhere in the surrounding environment, as demonstrated in both the ARPEGE-SH and HAMSTRAD data sets.

3.3. Potential Temperature Gradient

We now consider the mechanisms that allow the SLW cloud to persist in a thin layer (about 100-m deep) around 500-600 m altitude. Even if the PBL gets thinner after 12:00 UTC, it is evident that a residual mixed layer remains above (see e.g. Figure 1.7 of Stull, 2012 and Figure 12 top of Ricaud et al., 2012). At the time scale of a whole day, we can define the transition between the PBL and the free troposphere either at the top of the mixed layer, when this layer exists, or at the top of the residual layer, when a stable layer develops close to the surface and decouples the residual mixed layer from the surface. The transition is therefore characterized by a local maximum of the potential temperature (θ) vertical gradient ($\partial\theta/\partial z$).

Figure 6 shows $\partial\theta/\partial z$ computed from ARPEGE-SH, with the evolution of the PBL top and the SLW cloud superposed. The SLW cloud, once appeared at the top of the PBL around 08:00 UTC, persists after 12:00 UTC in a layer around 500-600 m coinciding with the local maximum of $\partial\theta/\partial z$, even after the PBL collapses down to the surface.

Figures 7a, b and c show the vertical profiles of θ (K) and $\partial\theta/\partial z$ (K km^{-1}) as calculated from temperature measured by the radiosondes and analysed by ARPEGE-SH at Dome C on

https://doi.org/10.5194/acp-2019-607
Preprint. Discussion started: 28 August 2019

24 December 2018 at 00:00 and 12:00 UTC and on 25 December 2018 at 00:00 UTC, respectively. The atmosphere as analysed by ARPEGE-SH is about 3-5 K warmer than the observations. From 100 m upward, the maximum of $\partial\theta/\partial z$ is measured at 400, 550 and 600 m on 24 December 2018 at 00:00 and 12:00 UTC and on 25 December 2018 at 00:00 UTC, respectively with an amplitude of 10, 12 and 40 K km^{-1}, respectively. This is broadly consistent with the ARPEGE-SH analyses though calculated maxima of $\partial\theta/\partial z$ (Fig. 7) are slightly higher (600, 700 and 600 m for the same dates, respectively) and less intense than those of radiosondes (8, 8 and 18 K km^{-1}, respectively).

The colocation of the positive potential temperature gradient with the height of the SLW clouds is consistent with the schematic representation of the diurnal variation of the PBL illustrated by Stull (2012) and adapted by Ricaud et al. (2012) for the Eastern Antarctic Plateau. Figure 8 is a modified version of Figure 12 from Ricaud et al. (2012) employing the naming conventions of Stull (2012). The layer where the clouds develop over the mixed layer is named the “entrainment zone” and the layer where the ice-water cloud persists over the residual quasi-mixed layer is named the “residual capping inversion” zone. These two zones are characterized by a positive $\partial\theta/\partial z$. Considering both the potential temperature gradients and the vertical extent of the SLW cloud, these layers are quite thin, less than 100-m deep.

Considering that the SLW clouds are so thin, they resemble stratocumulus, as can be observed at middle latitudes. The diurnal cycle of the SLW cloud also evokes that of oceanic stratocumulus, with a trend to fragmentation and/or dissipation during the “day” (local noon) because of solar absorption and to a solid deck state during the “night” (local midnight) because of reversed buoyancy due to cloud top longwave cooling. We use here the “night” and “day” terms for convenience, though solar radiation remains positive 24-hr long at this period of the year. During the YOPP intensive observing period, SLW clouds were observed for several days but it is not yet evident whether they were formed during the “day” (local noon) when the mixed

https://doi.org/10.5194/acp-2019-607
Preprint. Discussion started: 28 August 2019

Atmospheric Chemistry and Physics Discussions

layer becomes thick enough to reach the condensation level, and vertically broadened during the "night", or created during the "night" (local midnight) and then dissipated during the coming "day". Complementary observations would be needed, in particular turbulence profiles from the surface to above the top of boundary-layer clouds, to determine what is the coupling/decoupling diurnal cycle of these clouds.

3.4. Net Surface Radiation

The presence of clouds over Dome C has a strong impact on the net surface radiation as demonstrated by Ricaud et al. (2017). Figure 9 shows the time evolution of the net surface radiation as measured by the BSRN instruments and as calculated by ARPEGE-SH on 24 December 2018, superimposed with SLW cloud height. We also show the time evolution of the difference between surface radiation (W m^{-2}) observed by BSRN and calculated by ARPEGE-SH on 24 December 2018, in longwave downward (LW↓), longwave upward (LW↑), shortwave downward (SW↓) and shortwave upward (SW↑) components, superimposed with LWP. We highlight 4 periods with images taken from the webcam installed on the shelter hosting the LIDAR and HAMSTRAD: a) at 00:25 UTC (cirrus clouds, no SLW cloud), b) at 03:56 UTC (cirrus clouds, no SLW cloud), c) at 09:46 UTC (SLW cloud) and d) at 17:20 UTC (SLW cloud). The net surface radiation shows maxima between 00:00 and 05:00 UTC (08:00-13:00 LT) and minima between 11:00 and 13:00 UTC (19:00-21:00 LT) in the ARPEGE-SH and BSRN time series. When SLW clouds are present in the observations (08:00-10:00, 12:00-19:00 and around 21:00 UTC), whilst absent in ARPEGE-SH, the measured net surface radiation is systematically greater than the simulated one by 20-30 W m^{-2}. As the SLW horizontal extent is about 280 km and persists over more than 12 hours (section 3.1), this discrepancy in the net surface radiation between observation and NWP model may have a strong impact on the calculation of the radiation budget over Antarctica. In the presence of SLW clouds

https://doi.org/10.5194/acp-2019-607
Preprint. Discussion started: 28 August 2019

after 12:00 UTC, this difference is mainly attributable to LW↓ component, BSRN values being 50 W m^{-2} greater than those of ARPEGE-SH. Thus, SLW clouds tend to radiate LW radiation toward the ground (like greenhouse gases), at a level higher than more transparent clouds like cirrus. Note that there are differences from -30 to +60 W m^{-2} between observed and calculated SW↓ and SW↑ components but this difference falls within ±10 W m^{-2} for the net SW surface radiation (SW↓ - SW↑).

4. Perturbed diurnal cycle of the PBL

In this section, we focus on the second case study, 20 December 2018, when the diurnal cycle of the PBL was perturbed by the sudden arrival of very moist, warm air of oceanic origin (see Ricaud et al., 2017) on 20 December 2018. We analyse how this episode affected the presence and evolution of SLW clouds.

4.1. Clouds

As in section 3.1, the high LIDAR backscatter ($\beta_c > 100\ \beta_{mol}$) and low depolarization (<5%) showed the presence of SLW clouds (Figures 10a, b and c, respectively). Before 13:00 UTC, there is no trace of any clouds above Dome C while from 13:00 to 23:00 UTC SLW clouds are detected between 200 and 600 m. On all panels, we also superimposed the PBL top calculated by the ARPEGE-SH model. We note that the PBL top does not drop to the surface after 12:00 UTC as on 24 December 2018 but rather remains between 100 and 200 m. Consistent with the conclusions derived from the observations of 24 December 2018, the SLW cloud, once present, stays just above the height of the PBL top.

The cloud fraction, ice water and liquid water mixing ratios (kg kg^{-1}) calculated by ARPEGE-SH on 20 December 2018 are shown in Figures 11a, b and c, respectively. Contrary to the observations, the model simulates mixed-phase clouds (maximum cloud fraction of

https://doi.org/10.5194/acp-2019-607
Preprint. Discussion started: 28 August 2019

~30%), mainly composed of ice, with very little liquid-water, prior to 12:00 UTC; from 00:00 to 06:00 UTC, the clouds are forecasted below the PBL top. After 12:00 UTC, clouds appear 1-2 hours later in the model than in the observations, at 14:00-15:00 UTC, just below the PBL top (maximum cloud fraction of ~100%). The modelled cloud is mainly composed of ice with some traces of SLW above the PBL around 15:00-16:00 UTC. We note the presence of high altitude cirrus (ice) clouds calculated by ARPEGE-SH after 12:00 UTC around 3-4 km height, while not observed likely because of a lack of LIDAR sensitivity. As on 24 December 2018, the model fails to reproduce the presence of SLW clouds observed by the LIDAR near the PBL top.

The diurnal evolutions of the TCI calculated by ARPEGE-SH, the LWP from HAMSTRAD and ARPEGE-SH, and the IWV from HAMSTRAD and ARPEGE-SH on 20 December 2018 are presented in Figures 12a, b and c, respectively, with the presence of SLW clouds derived from the LIDAR observations superimposed on Fig. 12b. Ice clouds are calculated by ARPEGE-SH mainly around 15:00-16:00 UTC, with TCI values comparable to those on 24 December 2018. SLW clouds are deduced from HAMSTRAD LWP between 13:00 and 23:00 UTC which coincides well with the SLW clouds observed by the LIDAR. LWP values observed during this episode are much higher than on 24 December 2018, with a maximum amount of ~50 g m^{-2} about 20 times greater than the one measured (~2-3 g m^{-2}) on that day. Again, the ARPEGE-SH LWP is negligible (~10^{3} times less than observations). In parallel with the rapid increase of LWP, IWV also jumps from ~0.5 to ~2.3 kg m^{-2} within one hour after 13:00 UTC. ARPEGE-SH also calculates an increase of IWV but lagged by one hour and much less intense (~1.3 kg m^{-2}). Additionally, the model produces a systematically dryer atmosphere compared to HAMSTRAD by about 0.5 kg m^{-2} after 16:00 UTC, although before the cloudy period that starts at 12:00 UTC, ARPEGE-SH and HAMSTRAD IWV are consistent to within ±0.2 kg m^{-2}.

https://doi.org/10.5194/acp-2019-607
Preprint. Discussion started: 28 August 2019

4.2. Temperature and water vapour

The diurnal variations of the temperature and water vapour anomalies on 20 December 2018 as calculated by ARPEGE-SH and measured by HAMSTRAD are shown in Figure 13. In ARPEGE-SH, a sharp transition between a warm and a cool atmosphere is evident at 12:00 UTC below the top of the PBL. In HAMSTRAD, from 00:00 to 06:00 UTC, the atmosphere starts warming and then from 06:00 to 13:00 UTC, cools gradually to a minimum. After 13:00 UTC, HAMSTRAD temperatures reveal a warming starting from the surface and progressively thickening until reaching the top of the PBL by the end of the day. Above the PBL, the HAMSTRAD-observed and ARPEGE-SH-calculated temporal evolution of temperature and water vapour are in an overall agreement. In the PBL, the model data show a moistening around 05:00 UTC, but the most striking event is a sudden drying at 12:00 UTC. In HAMSTRAD, there is a continuous drying from 00:00 UTC, followed by an obvious transition at 13:00 UTC, opposite to that of ARPEGE-SH at 12:00 UTC. The warm and wet atmosphere observed after 13:00 UTC develops a mixed layer, consequently the PBL top no longer collapses to a stable layer, in contrast to what was observed on 24 December. Furthermore, the SLW clouds present in the entrainment zone steadily remain at the PBL top until the end of the day.

4.3. Potential Temperature Gradient

Figure 14 shows $\partial\theta/\partial z$ (K km^{-1}) from ARPEGE-SH, with the evolution of the PBL top and the SLW cloud superimposed. In these perturbed conditions, the SLW clouds are present a few tens of meters above the top of the PBL after 12:00 UTC. The PBL top is located in a layer coinciding with the local maximum of $\partial\theta/\partial z$, around 100-300 m, and does not dramatically decrease to the surface for the rest of the day.

https://doi.org/10.5194/acp-2019-607
Preprint. Discussion started: 28 August 2019

Atmospheric Chemistry and Physics Discussions
Open Access

Figures 15a, b and c show the vertical profiles of θ (K) and ∂θ/∂z (K km^{-1}) as calculated from temperature measured by the radiosondes and analysed by ARPEGE-SH at Dome C on 20 December 2018 at 00:00 and 12:00 UTC and on 21 December 2018 at 00:00 UTC, respectively. The ARPEGE-SH profiles are about 0-5 K warmer than the observations. From 50 m upward, the maximum of ∂θ/∂z is measured at 75, 150 and 375 m on 20 December 2018 at 00:00 and 12:00 UTC and on 21 December 2018 at 00:00 UTC, respectively, with a corresponding amplitude of 75, 40 and 55 K km^{-1}. This is broadly consistent with the ARPEGE-SH calculations on 20 December 2018 prior to the warm and wet episode: at 00:00 UTC (Fig. 15a), the calculated ∂θ/∂z is maximum at 75 m and reaches 100 K km^{-1}, whereas at 12:00 UTC (Fig. 15b) it peaks at 200 m (slightly higher than observed) with a value of 50 K km^{-1}. After the warm and wet episode on 21 December 2018 at 00:00 UTC (Fig. 15c), the vertical profile of ∂θ/∂z calculated by ARPEGE-SH shows two maxima at 100 and 450 m with an amplitude of 45 and 25 K km^{-1}, respectively, that strongly differ from the observations.

4.4. Net Surface Radiation

Figure 16 shows the net surface radiation as measured by the BSRN photometric instruments and as calculated by ARPEGE-SH for 20 December 2018, superimposed with the SLW clouds. We also show the time evolution of difference in surface radiation (W m^{-2}) observed by BSRN and calculated by ARPEGE-SH on 20 December 2018 for LW↓, LW↑, SW↓ and SW↑ components, superimposed with LWP. We highlight 4 periods with snapshots taken from the webcam: 1) 07:15 UTC (clear sky), 2) 12:35 UTC (clear sky), 3) 13:30 UTC (SLW cloud) and 4) 21:00 UTC (SLW cloud). Before 13:00 UTC, there are no clouds above Dome C whilst after 13:00 UTC clouds are present. The diurnal evolution of the modelled and observed net surface radiation shows a maximum of ~+50 W m^{-2} in ARPEGE-SH and ~+85 W m^{-2} in BSRN over the period 00:00-04:00 UTC and a minimum of about -50 W m^{-2} around

https://doi.org/10.5194/acp-2019-607
Preprint. Discussion started: 28 August 2019

12:00-13:00 UTC on both time series. Nevertheless, when SLW clouds are observed at 13:00 UTC, the observed net surface radiation jumps to +10 W m^{-2}, a feature not reproduced in the model. The difference between the BSRN-observed and ARPEGE-SH-modelled net surface radiation is larger than +30 W m^{-2} when SLW clouds are present, reaching +60 W m^{-2} when the LWP measured by HAMSTRAD is at its maximum (50 g m^{-2} at 13:00 UTC). This is twice the difference observed in the non-perturbed PBL episode detailed in section 3.4. This underlines again the strong impact SLW clouds may have on the radiation budget over Antarctica. In the presence of SLW clouds after 13:00 UTC, the difference in net surface radiation is mainly attributable to LW↓ component, BSRN values being 100 W m^{-2} greater than those of ARPEGE-SH. Note that there are differences from -100 to +60 W m^{-2} between observed and calculated SW↓ and SW↑ components but this difference falls below 20 W m^{-2} for the net SW surface radiation (SW↓ - SW↑).

5. Conclusions

A comprehensive water budget study has been performed during the YOPP international campaign held at Dome C (Concordia, Antarctica) from mid-November 2018 to mid-February 2019. Supercooled liquid water (SLW) clouds were observed and analysed by means of remote-sensing ground-based instrumentation (tropospheric depolarization LIDAR, HAMSTRAD microwave radiometer, BSRN net surface radiation), radiosondes, spaceborne sensor (CALIOP/CALIPSO depolarization LIDAR) and the NWP ARPEGE-SH. The analyses focused on two periods showing 1) a "typical" diurnal cycle of the PBL on 24 December 2018 (warm and dry, local mixing layer followed by a thinner cold and dry, local stable layer which develops when the surface has cooled down) and 2) a perturbed diurnal cycle of the PBL on 20 December 2018 (a warm and wet episode prevented from a clear diurnal cycle of the PBL top).

https://doi.org/10.5194/acp-2019-607
Preprint. Discussion started: 28 August 2019

Whatever the state of the diurnal cycle of the PBL top (typical or perturbed), thin (~100-m thick) SLW clouds have been observed by ground-based and spaceborne LIDARs developing within the entrainment and the capping inversion zones at the top of the PBL. Spaceborne lidar observations revealed horizontal extensions of these clouds as large as 280 and 550 km for the 24 and 20 December cases, respectively. ARPEGE-SH was not able to correctly estimate the ratio between liquid and solid water inside the cloudy layers, with SLW always strongly underestimated in the studied cases. Consequently, the net surface radiation was affected by the presence of SLW clouds during these two episodes. The net surface radiation observed by BSRN was 20-30 W m^{-2} higher than that modelled in ARPEGE-SH on 24 December 2018 (typical diurnal cycle of the PBL), this difference reaching +50 W m^{-2} on 20 December 2018 (perturbed diurnal cycle of the PBL), consistent with the total observed liquid water being 20 times greater in the perturbed PBL diurnal cycle than in the typical PBL diurnal cycle. The difference in the net surface radiation is mainly attributable to longwave downward surface radiation, BSRN values being 50 and 100 W m^{-2} greater than those of ARPEGE-SH in the typical and perturbed cases, respectively.

Time coincident ground-based remote-sensed measurements of water (vapour, liquid and solid), temperature and net surface radiation are available at Dome C since 2015. Consequently, a comprehensive statistical analysis of the presence of SLW clouds will be performed in the near future. Coupled with modelling studies (NWP ARPEGE-SH, mesoscale models), an estimation of the radiative impact of these clouds on the local climate will then be performed.

Data availability

HAMSTRAD data are available at http://www.cnrm.meteo.fr/spip.php?article961&lang=en (last access: 28 August 2019). The CALIOP images are accessible at http://www-calipso.larc.nasa.gov/ (last access: 28 August 2019). The tropospheric depolarization LIDAR data are reachable at http://lidarmax.altervista.org/englidar/_Antarctic%20LIDAR.php (last access: 28 August 2019). Radiosondes are available at http://www.climantartide.it (last access: 28 August 2019). BSRN data can be obtained from the ftp server (https://bsrn.awi.de/data/data-retrieval-via-ftp/) (last access: 28 August 2019). The ARPEGE data and corresponding technical information are available from the YOPP Data Portal and from the ftp server (ftp.umr-cnrm.fr with user: yopp and password: Arpege) (last access: 28 August 2019).

Author contributions

PR, MDG, AL, and PG provided the observational data while EB, NA and VG developed the model code and performed the simulations. PD, JLA and DV contributed to the data interpretation. All the co-authors participated in the data analysis. PR prepared the manuscript with contributions from all co-authors.

Competing interests

The authors declare that they have no conflict of interest.

Acknowledgments

The present research project Water Budget over Dome C (H2O-DC) has been approved by the Year of Polar Prediction (YOPP) international committee. The HAMSTRAD programme (910) was supported by the French Polar Institute, Institut polaire français Paul-Emile Victor (IPEV), the Institut National des Sciences de l'Univers (INSU)/Centre National de la Recherche Scientifique (CNRS), Météo-France and the Centre National d'Etudes Spatiales (CNES). The permanently manned Concordia station is jointly operated by IPEV and the Italian Programma Nazionale Ricerche in Antartide (PNRA). The tropospheric LIDAR operates at Dome C from 2008 within the framework of several Italian national (PNRA) projects. We would like to thank all the winterover personnel who worked at Dome C on the different projects: HAMSTRAD, aerosol LIDAR and BSRN. The authors also acknowledge the CALIPSO science team for providing the CALIOP images.

References

Adhikari, L., Wang, Z. and Deng, M.: Seasonal variations of Antarctic clouds observed by CloudSat and CALIPSO satellites, J. Geophys. Res., 117, D04202, doi:10.1029/2011JD016719, 2012.

Argentini, S., Viola, A., Sempreviva, A. M. and Petenko, I.: Summer boundary-layer height at the plateau site of Dome C, Antarctica, Bound.-Layer Meteor., 115, 409-422, 2005.

Bromwich, D. H., Nicolas, J. P., Hines, K. M., Kay, J. E., Key, E. L., Lazzara, M. A., ... & Lachlan-Cope, T. (2012). Tropospheric clouds in Antarctica. Reviews of Geophysics, 50(1).

Bromwich, D. H., Otieno, F. O., Hines, K. M., Manning, K. W., & Shilo, E. (2013). Comprehensive evaluation of polar weather research and forecasting model performance in the Antarctic. Journal of Geophysical Research: Atmospheres, 118(2), 274-292.

Casasanta, G., Pietroni, I., Petenko, I., and Argentini, S.: Observed and modelled convective mixing-layer height at Dome C, Antarctica, Boundary-layer meteorology, 151(3), 597-608, 2014.

Driemel, A., Augustine, J., Behrens, K., Colle, S., Cox, C., Cuevas-Agulló, E., et al.: Baseline Surface Radiation Network (BSRN): structure and data description (1992–2017), Earth Syst. Sci. Data, 10, 1491-1501, https://doi.org/10.5194/essd-10-1491-2018, 2018.

Goy, C., Potenza, M. A., Dedera, S., Tomut, M., Guillerm, E., Kalinin, A., ... and Tejeda, G.: Shrinking of rapidly evaporating water microdroplets reveals their extreme supercooling. Physical review letters, 120(1), 015501, 2018.

https://doi.org/10.5194/acp-2019-607
Preprint. Discussion started: 28 August 2019

Hogan, R. J., and Illingworth, A. J.: The effect of specular reflection on spaceborne lidar measurements of ice clouds. Report of the ESA Retrieval algorithm for EarthCARE project, 2003.

King, J. C., Argentini, S. A., & Anderson, P. S. (2006). Contrasts between the summertime surface energy balance and boundary layer structure at Dome C and Halley stations, Antarctica. Journal of Geophysical Research: Atmospheres, 111(D2).

Lachlan-Cope, T. (2010). Antarctic clouds. Polar Research, 29(2), 150-158.

Lawson, R. P., & Gettelman, A. (2014). Impact of Antarctic mixed-phase clouds on climate. Proceedings of the National Academy of Sciences, 111(51), 18156-18161.

Listowski, C., Delanoë, J., Kirchgaessner, A., Lachlan-Cope, T., and King, J.: Antarctic clouds, supercooled liquid water and mixed-phase investigated with DARDAR: geographical and seasonal variations, Atmos. Chem. Phys. Discuss., https://doi.org/10.5194/acp-2018-1222, in review, 2018.

Lubin, D., Chen, B., Bromwich, D. H., Somerville, R. C., Lee, W. H., and Hines, K. M.: The Impact of Antarctic Cloud Radiative Properties on a GCM Climate Simulation, J. Climate, 11, 447-462, 1998.

Mishchenko, M. I., J. W. Hovenier, and L. D. Travis (Eds.): Light Scattering by Nonspherical Particles: Theory, Measurements, and Applications. Academic Press. Chapter 14, 393-416, 2000.

Pailleux, J., Geleyn, J.-F., El Khatib, R., Fischer, C., Hamrud, M., Thépaut, J.-N., et al. (2015). Les 25 ans du système de prévision numérique du temps IFS/Arpège, *La Météorologie*, 89, 18-27, http://hdl.handle.net/2042/56594, DOI : https://doi.org/10.4267/2042/56594

Palchetti, L., Bianchini, G., Di Natale, G., and Del Guasta, M.: Far infrared radiative properties of water vapor and clouds in Antarctica, B. Am. Meteorol. Soc., 96, 1505-1518, doi:10.1175/BAMS-D-13-00286.1, 2015.

https://doi.org/10.5194/acp-2019-607
Preprint. Discussion started: 28 August 2019

Pruppacher, H. R., and Klett, J. D.: Microphysics of Clouds and Precipitation: Reprinted 1980. Springer Science & Business Media, 2012.

Ricaud, P., Gabard, B., Derrien, S., Chaboureau, J.-P., Rose, T., Mombauer, A. and Czekala, H.: HAMSTRAD-Tropo, A 183-GHz Radiometer Dedicated to Sound Tropospheric Water Vapor Over Concordia Station, Antarctica, IEEE Trans Geosci Remote Sens., 48, 1365–1380, doi: 10.1109/TGRS.2009.2029345, 2010a.

Ricaud, P., B., Gabard, S. Derrien, J.-L. Attié, T. Rose, and H. Czekala, Validation of tropospheric water vapor as measured by the 183-GHz HAMSTRAD Radiometer over the Pyrenees Mountains, France, IEEE Transactions on Geoscience and Remote Sensing, Vol. 48, No. 5, 2189-2203, 2010b.

Ricaud, P., Genthon, C., Durand, P., Attié, J.-L., Carminati, F., Canut, G., Vanacker, J.-F., Moggio, L., Courcoux, Y., Pellegrini, A. and Rose, T.: Summer to Winter Diurnal Variabilities of Temperature and Water Vapor in the lowermost troposphere as observed by the HAMSTRAD Radiometer over Dome C, Antarctica, Bound.-Layer Meteor., 143, 227–259, doi:10.1007/s10546-011-9673-6, 2012.

Ricaud, P., Grigioni, P., Zbinden, R., Attié, J.-L., Genoni, L., Galeandro, A., Moggio, A., Montaguti, S., Petenko, I. and Legovini, P.: Review of tropospheric temperature, absolute humidity and integrated water vapour from the HAMSTRAD radiometer installed at Dome C, Antarctica, 2009–14, Antarct. Sci., 27, 598-616, doi:10.1017/S0954102015000334, 2015.

Ricaud, P., Bazile, E., del Guasta, M., Lanconelli, C., Grigioni, P., and Mahjoub, A.: Genesis of diamond dust, ice fog and thick cloud episodes observed and modelled above Dome C, Antarctica, Atmos. Chem. Phys., 17, 5221-5237, doi:10.5194/acp-17-5221-2017, 2017.

Stull, R. B.: An introduction to boundary layer meteorology (Vol. 13). Springer Science & Business Media, 2012.

https://doi.org/10.5194/acp-2019-607
Preprint. Discussion started: 28 August 2019

Tomasi, C., Petkov, B., Mazzola, M., Ritter, C., di Sarra, A., di Iorio, T., and del Guasta, M.: Seasonal variations of the relative optical air mass function for background aerosol and thin cirrus clouds at Arctic and Antarctic sites, Remote Sensing, 7(6), 7157-7180, 2015.

Winker, D. M., Vaughan, M. A., Omar, A., Hu, Y., Powell, K. A., Liu, Z., Hunt, W. H. and Young, S. A.: Overview of the CALIPSO mission and CALIOP data processing algorithms, J. Atmos. Oceanic Technol., 26, 2310-2323, 2009.

Young, S. A. and Vaughan, M. A.: The retrieval of profiles of particulate extinction from Cloud Aerosol Lidar Infrared Pathfinder Satellite Observations (CALIPSO) lidar data: Algorithm description, J. Atmos. Oceanic Technol., 26, 1105–1119, 2009.

https://doi.org/10.5194/acp-2019-607
Preprint. Discussion started: 28 August 2019

Atmospheric Chemistry and Physics Discussions
Open Access
EGU

Figures

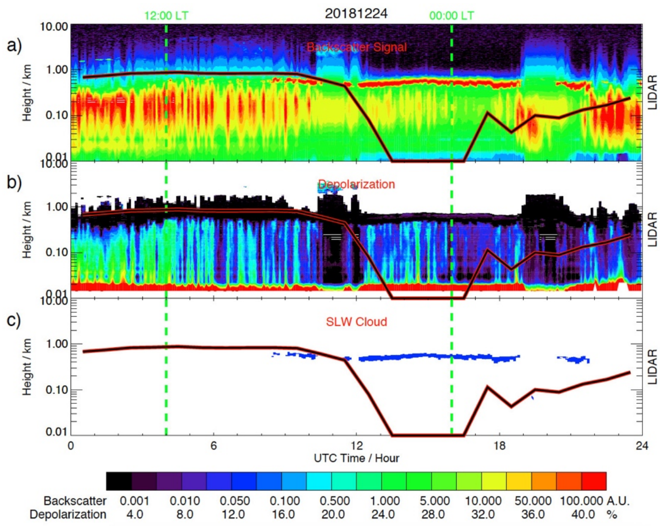

Figure 1: Diurnal variation on 24 December 2018 (UTC Time) along the vertical of: a) the backscatter signal (Arbitrary Unit, A.U.), b) the depolarization ratio (%) measured by the aerosol LIDAR, and c) the Supercooled Liquid Water (SLW) cloud height (blue) deduced from the aerosol LIDAR ($\beta_c > 100\ \beta_{mol}$, depolarization < 5%). Superimposed to all the Figures is the top of the Planetary Boundary Layer calculated by the ARPEGE-SH model (black-red thick line). Two vertical green dashed lines indicate 12:00 and 00:00 LT.

Atmospheric Chemistry and Physics
Discussions

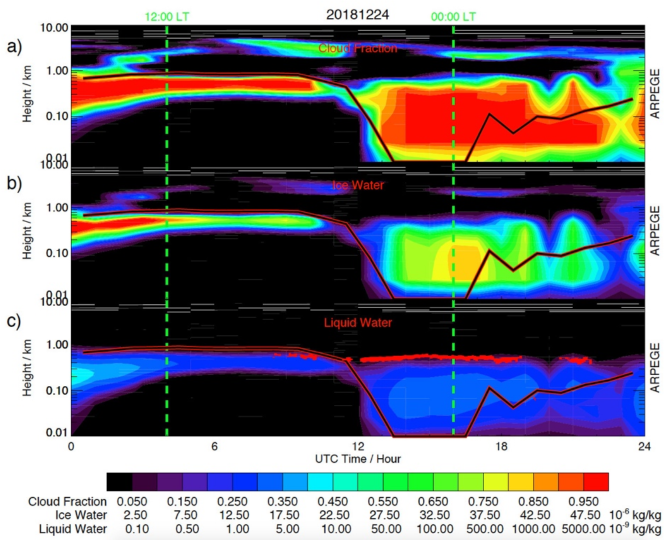

Figure 2: Time-height cross section on 24 December 2018 (UTC Time) of: a) the Cloud Fraction (0-1), b) the Ice Water mixing ratio (10^{-6} kg kg^{-1}) and c) the Liquid Water mixing ratio (10^{-6} kg kg^{-1}) calculated by the ARPEGE-SH model. Superimposed to all the panels is the top of the Planetary Boundary Layer calculated by the ARPEGE-SH model (black-red thick line). Superimposed in panel c is the SLW cloud (red area) height depth deduced from the LIDAR observations (see Fig. 1c). Two vertical green dashed lines indicate 12:00 and 00:00 LT.

https://doi.org/10.5194/acp-2019-607
Preprint. Discussion started: 28 August 2019

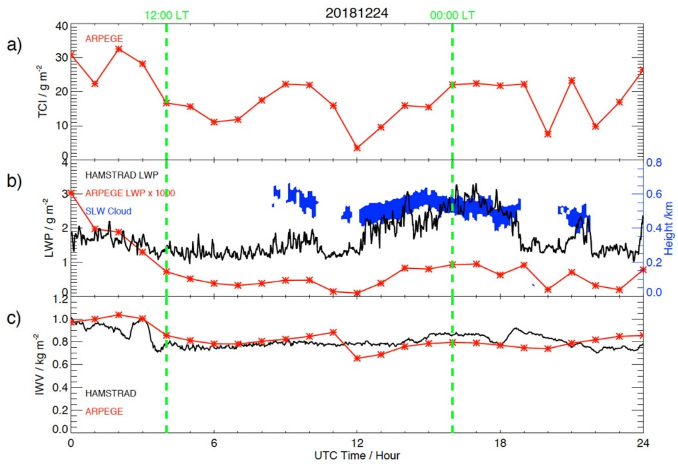

Figure 3: Diurnal variation on 24 December 2018 (UTC Time) of: a) the Total Column of Ice (TCI) (g m^{-2}) calculated by ARPEGE-SH (red crossed line), b) the Liquid Water Path (LWP) measured by HAMSTRAD (g m^{-2}, black solid line) and calculated by ARPEGE-SH (x1000 g m^{-2}, red crossed line) and c) the Integrated Water Vapour (IWV, kg m^{-2}) measured by HAMSTRAD (black solid line) and calculated by ARPEGE-SH (red crossed line). Superimposed to panel b) is the SLW cloud thickness (blue area) deduced from the LIDAR observations (see Fig. 1c) (blue y-axis on the right of the Figure). Note LWP from ARPEGE-SH has been multiplied by a factor 1000. Two vertical green dashed lines indicate 12:00 and 00:00 LT.

https://doi.org/10.5194/acp-2019-607
Preprint. Discussion started: 28 August 2019

Atmospheric Chemistry and Physics Discussions

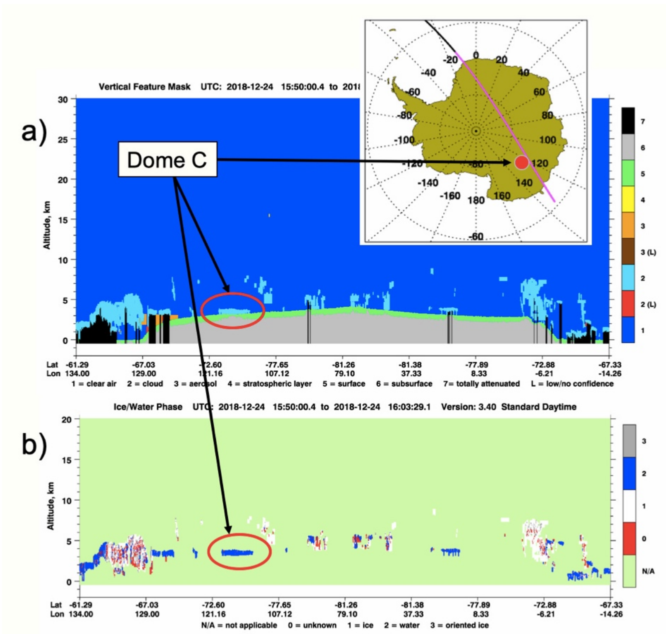

Figure 4: CALIOP/CALIPSO spaceborne LIDAR observations along one orbit on 24 December 2018 (15:50-16:00 UTC) in the vicinity of Dome C (75°S, 123°E): a) the Vertical Feature Mask highlighting a cloud (light blue) near the surface (red circle) and b) the Ice/Water Phase Mask highlighting a SLW (dark blue) cloud near the surface (red circle). The ground-track of the sensor (pink) has been embedded at the top of the Figure, with the location of Dome C marked (red filled circle). Note that the altitude is relative to the sea surface, with the height of surface of Dome C at an elevation of 3233 m amsl.

https://doi.org/10.5194/acp-2019-607
Preprint. Discussion started: 28 August 2019

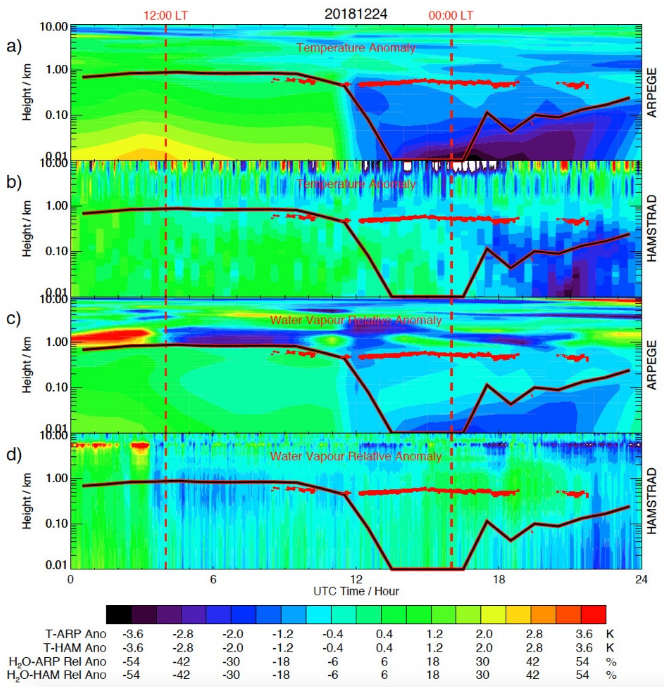

Figure 5: Time-height cross section on 24 December 2018 (UTC Time) of a) the temperature anomaly (K) and b) the water vapour relative anomaly (%) calculated by ARPEGE-SH, c) the temperature anomaly (K) and d) the water vapour relative anomaly (%) observed by HAMSTRAD. Superimposed to all the Figures are the SLW cloud altitude (red area) deduced from the LIDAR observations (see Fig. 1c) and the top of the Planetary Boundary Layer calculated by the ARPEGE-SH model (black-red thick line). Two vertical red dashed lines indicate 12:00 and 00:00 LT.

https://doi.org/10.5194/acp-2019-607
Preprint. Discussion started: 28 August 2019

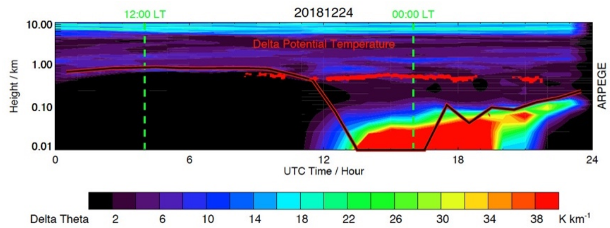

Figure 6: Time-height cross section of $\partial\theta/\partial z$ (K km^{-1}) calculated from ARPEGE-SH temperature on 24 December 2018 (UTC Time). Superimposed are the SLW cloud altitude (red area) deduced from the LIDAR observations (see Fig. 1) and the top of the Planetary Boundary Layer calculated by the ARPEGE-SH model (black-red thick line). Two vertical green dashed lines indicate 12:00 and 00:00 LT.

https://doi.org/10.5194/acp-2019-607
Preprint. Discussion started: 28 August 2019

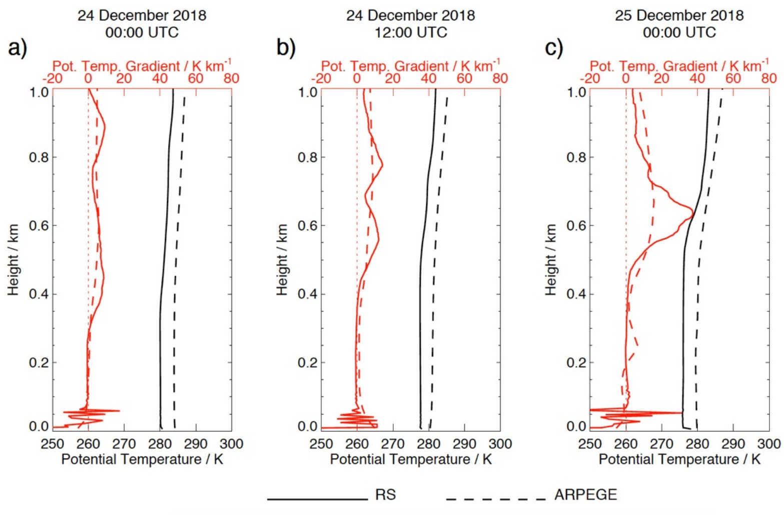

Figure 7: Vertical profiles of potential temperature θ (black) and the gradient in potential temperature ∂θ/∂z (red) as calculated from temperature measured by the radiosondes (solid line) and analysed by ARPEGE-SH (dashed line) at Dome C on 24 December 2018 at a) 00:00 and b) 12:00 UTC, and c) on 25 December 2018 at 00:00 UTC.

https://doi.org/10.5194/acp-2019-607
Preprint. Discussion started: 28 August 2019

Atmospheric Chemistry and Physics Discussions

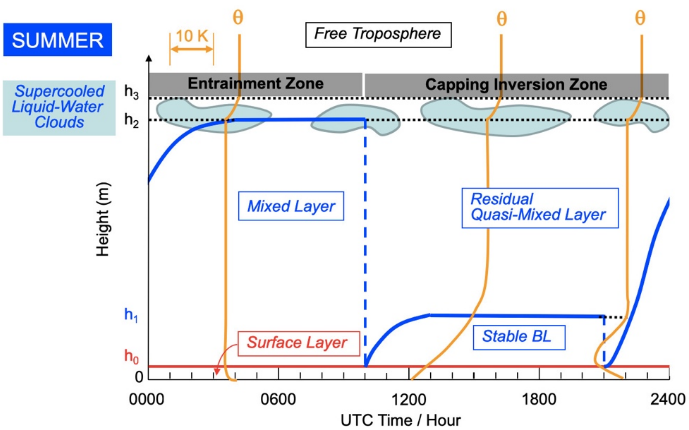

Figure 8: Figure modified and updated from Fig. 12 of Ricaud et al. (2012) showing the diurnal evolution (UTC Time) of the different layers in the Planetary Boundary Layer (PBL) with h_0 the top of the surface layer, h_2 the daily overall top of the PBL, and h_1 the top of the intermediate stable layer within the PBL. The orange lines symbolize the vertical profiles of potential temperature θ. The layer between h_2 and h_3 is named "entrainment zone" above the mixed layer and "capping inversion zone" elsewhere. h_3 represents the top of this layer. SLW clouds are represented within this layer. Note that LT = UTC + 8 h.

https://doi.org/10.5194/acp-2019-607
Preprint. Discussion started: 28 August 2019

Atmospheric Chemistry and Physics Discussions

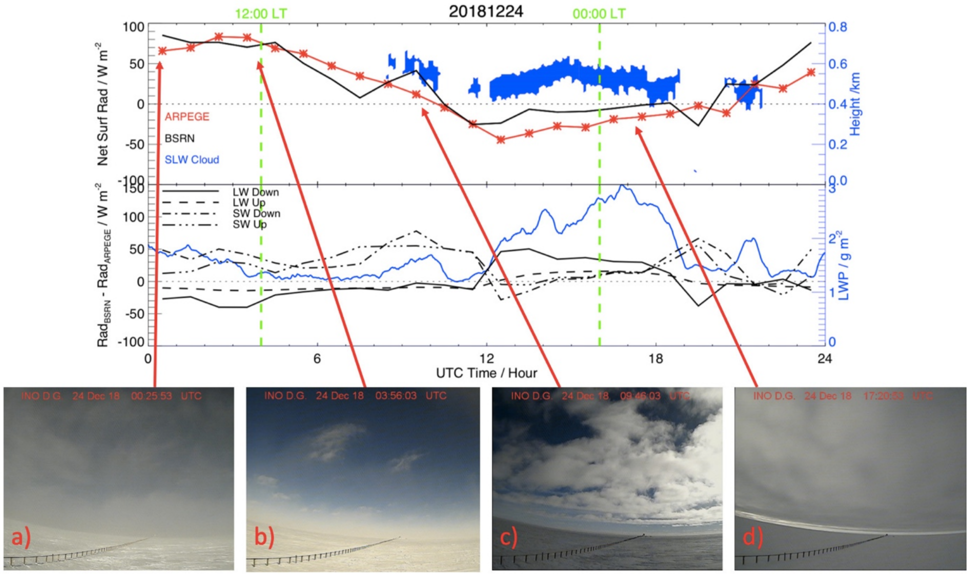

Figure 9: (Top) Diurnal variation of the net surface radiation (W m^{-2}) observed by BSRN (black solid line) and calculated by ARPEGE-SH (red crossed line) on 24 December 2018 in UTC Time. Superimposed is the SLW cloud altitude (blue) deduced from the LIDAR. (Middle) Diurnal variation of the difference between surface radiation (W m^{-2}) observed by BSRN and calculated by ARPEGE-SH on 24 December 2018 for longwave downward (black solid), longwave upward (black dashed), shortwave downward (black dashed dotted) and shortwave upward (black dashed triple dotted) components. Superimposed is LWP (blue) measured by HAMSTRAD. (Bottom) Four webcam images showing the cloud coverage at: a) 00:25 UTC and b) 03:56 UTC (cirrus clouds, no SLW cloud), c) 09:46 UTC (SLW cloud) and d) 17:20 UTC (SLW cloud). Two vertical green dashed lines indicate 12:00 and 00:00 LT.

https://doi.org/10.5194/acp-2019-607
Preprint. Discussion started: 28 August 2019

Atmospheric Chemistry and Physics
Discussions

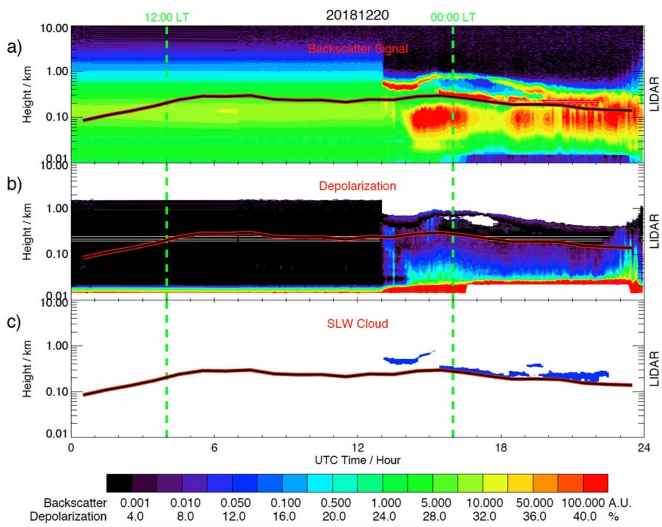

Figure 10: Same as Figure 1 but for 20 December 2018.

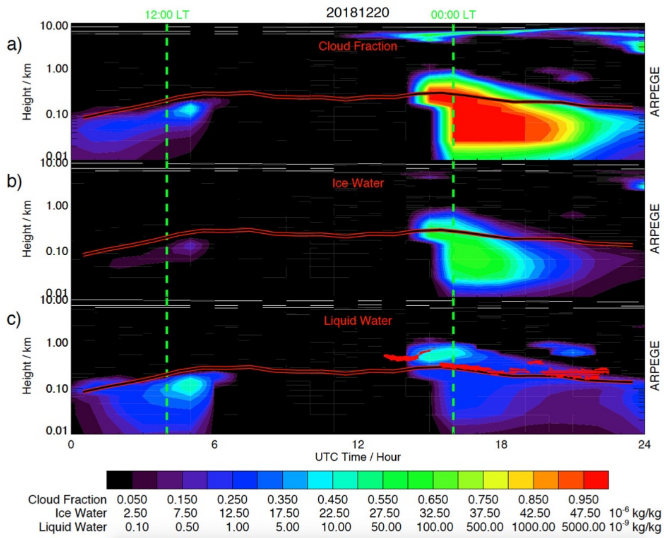

Figure 11: Same as Figure 2 but for 20 December 2018.

https://doi.org/10.5194/acp-2019-607
Preprint. Discussion started: 28 August 2019

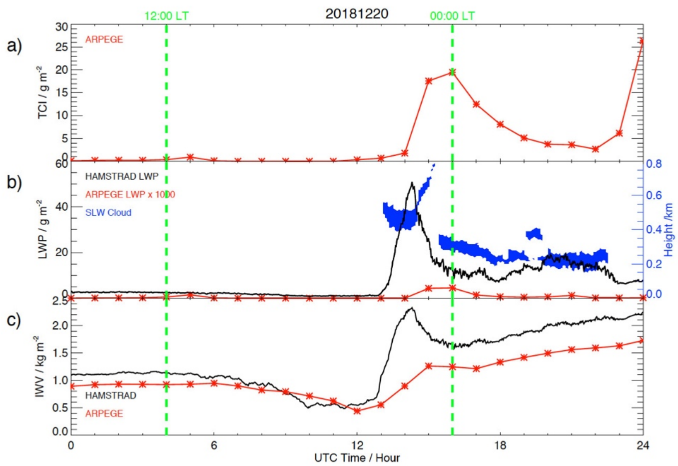

Figure 12: Same as Figure 3 but for 20 December 2018.

https://doi.org/10.5194/acp-2019-607
Preprint. Discussion started: 28 August 2019

723 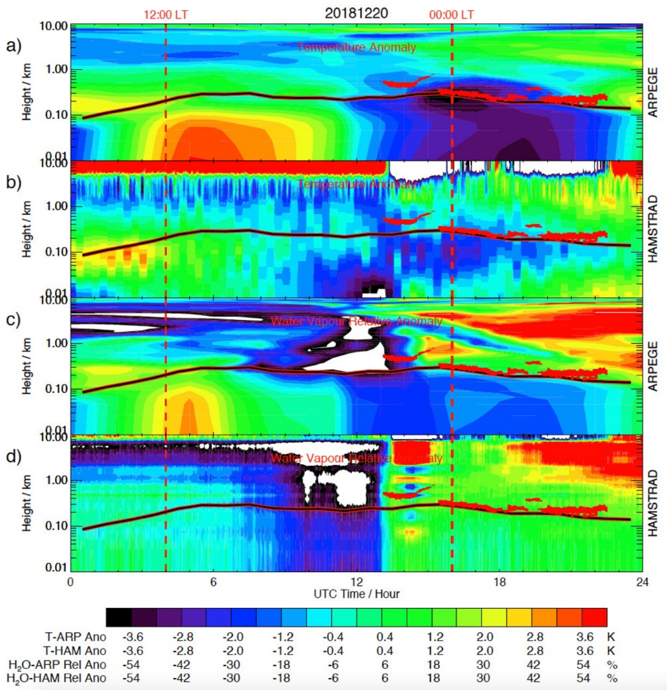

724 **Figure 13:** Same as Figure 5 but for 20 December 2018.

725
726

https://doi.org/10.5194/acp-2019-607
Preprint. Discussion started: 28 August 2019

Atmospheric Chemistry and Physics
Discussions

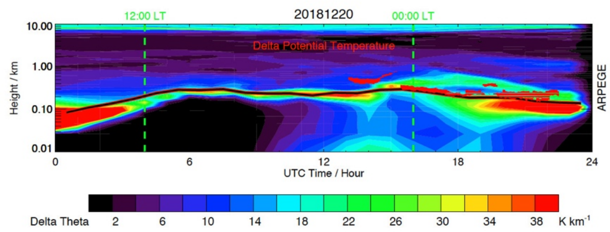

Figure 14: Same as Figure 6 but for 20 December 2018.

https://doi.org/10.5194/acp-2019-607
Preprint. Discussion started: 28 August 2019

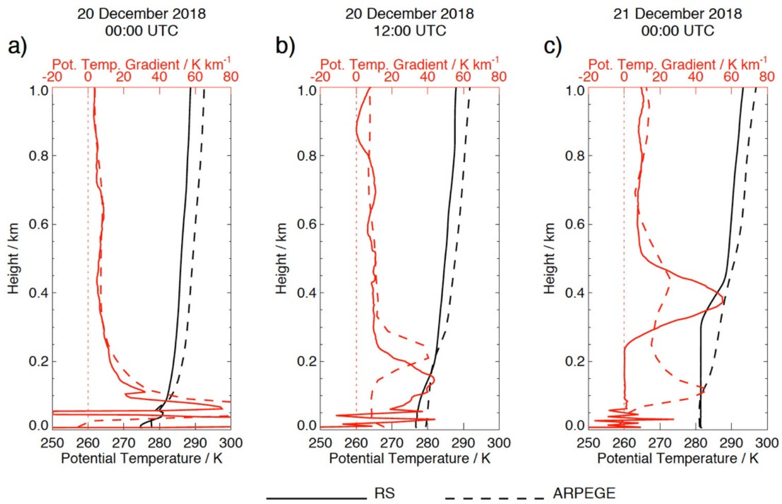

732

733 **Figure 15:** Same as Figure 7 but on 20 December 2018 at a) 00:00 and b) 12:00 UTC, and c)

734 on 21 December 2018 at 00:00 UTC.

735

736

https://doi.org/10.5194/acp-2019-607
Preprint. Discussion started: 28 August 2019

Atmospheric Chemistry and Physics Discussions

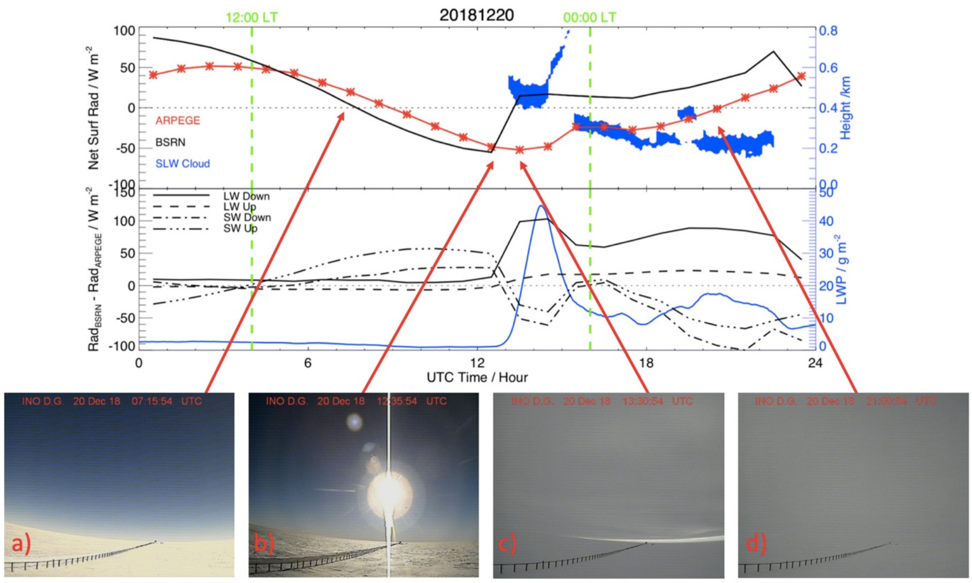

Figure 16: Same as Figure 9 but for 20 December 2018 whilst the 4 webcam images were selected at: a) 07:15 and b) 12:35 UTC (clear sky), c) 13:30 and d) 21:00 UTC (SLW cloud).